Anaesthetic Mechanism on a Model Biological Membrane: A Molecular Dynamics Simulation Study

J. J. López Cascales, J. G. Hernández Cifre, and J. García de la Torre*

Departamento de Química Física, Universidad de Murcia, Campus de Espinardo 30071, Murcia, Spain

Received: April 30, 1997; In Final Form: October 21, 1997[⊗]

We study the effects of anaesthetic molecules at surgical concentration on a biological membrane model, in an attempt to elucidate the mechanism by which the anaesthetic interacts with the membrane. Using a molecular dynamics simulation of benzyl alcohol molecules embedded in a lipid membrane, we detected no relevant structural change in the hydrocarbon region of the membrane that might explain the action mechanism of the anaesthetic. Only a slight increase in the disorder of the membrane in the deepest zones of the hydrocarbon region was measured from our simulations in the presence of benzyl alcohol. No variation in the thickness of the membrane, surface area per lipid molecule, or atom distribution across the membrane was detected from our simulations when the anaesthetic was embedded in the interior of the membrane. On the other hand, there was clear anisotropy in the rotational and translational diffusion coefficients of the benzyl alcohol molecules in the interior of the membrane.

1. Introduction

How anaesthetics act on biological membranes is a subject that remains unclear after almost a century of thorough investigations.[1−7] Two different mechanisms have been proposed, the first of which deals with the alterations introduced by the presence of anaesthetics in the structure of a lipid membrane, while the second one suggests that anaesthetics have a direct bearing on the function of the proteins embedded in the membrane.[7]

We decided to focus our interest on the perturbing effects of anaesthetics on the membrane, with the aim of identifying the real effect of the presence of these anaesthetic molecules at surgical concentrations on the lipid membrane structure. With such a goal, a biological membrane was modeled as a lipid bilayer of dimyristoylphosphatidylcholine (DMPC) containing benzyl alcohol (Ph−CH_2−OH) as the anaesthetic. Benzyl alcohol was selected for this study mainly because it is widely used in surgery, but also because of the amount of experimental data for the DMPC/benzyl alcohol system that there are available in the literature.[1−3]

The technique of molecular dynamics simulation has been widely used to study lipid membranes,[8−16] principally because of the serious problems associated with experimental studies using X-ray or NMR of systems with no well-defined structure (as in the case of the biological membranes). Moreover, other techniques, such as the fluorescent anisotropy decay of dye molecules embedded in lipid bilayers,[7,17] may disrupt the real structure of the membrane.[18] Molecular dynamics simulations, on the other hand, afford valuable information that permits us to obtain an insight into lipid membranes at the atomic level, without using extra molecules which might perturb the native state of the membrane system.

We also focused our interest on the dynamic properties of the benzyl alcohol molecules in the interior of lipid membranes. We anticipated that we would observe a great lack of homogeneity in the hydrocarbon region, in the sense that most of the dynamic properties of the anaesthetic molecules are very dependent on their position in the interior of the membrane.

2. Method and Models

Building Up the System. The lipid bilayer model was built up from the structure of a single lipid molecule of DMPC generated using the HyperChem commercial package.[19] The lipid molecule was replicated 72 times to give a bilayer containing two leaflets of 36 lipids each, with the lipids separated in such a way that the mean surface area per lipid was about 64 Å^2, corresponding to the experimental value associated with a DMPC membrane in its liquid crystalline state.[20] The united atom model (no hydrogens) was employed for the lipid molecules. Above and below the lipid bilayer, two 1.5 nm thick layers of water were added to the system, which amount to 1444 water molecules, by copying an equilibrated box containing 216 molecules of the SPC water model.[21] Periodic boundary conditions were applied to the repeating box thus obtained.

The charge distribution on a single lipid molecule of DMPC was taken from ref 22 and is displayed in Figure 1 with the atom numeration that will be used in this work. As regards the benzyl alcohol molecule, the charge and structure of this molecule were generated using the HyperChem package.[19] Three benzyl alcohol molecules were introduced in the repeating box, which gave a DMPC:alcohol ratio of 24:1 similar to surgical levels. The structure of a single molecule of benzyl alcohol was replicated three times and manually introduced into the middle of the hydrocarbon region of the lipid bilayer. The locations of the molecules were chosen arbitrarily, although case was taken that their positions and orientations differed. Figure 2 displays the charge and the atom numeration of a benzyl alcohol molecule.

After construction of the whole system, its total energy was minimized in order to remove undesired overlaps between adjacent atoms. Figure 3 displays a snapshot of the whole system along the trajectory taken in the middle of the simulation.

* To whom correspondence should be addressed. e-mail: jgt@fcu.um.es.
[⊗] Abstract published in *Advance ACS Abstracts,* December 15, 1997.

S1089-5647(97)01453-3 CCC: $15.00
Published on Web 01/15/1998

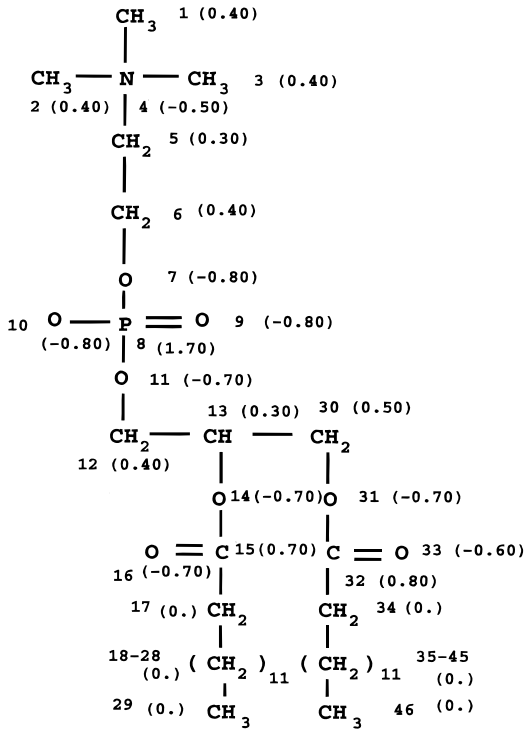

Figure 1. Atom numeration and charge distribution on a DMPC molecule.

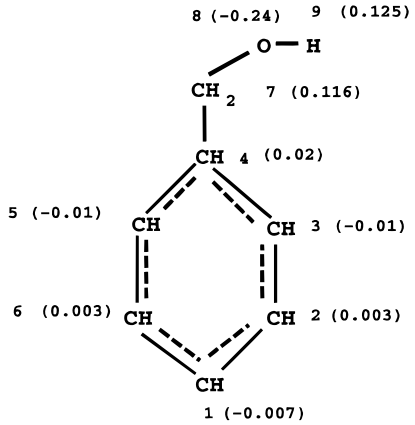

Figure 2. Atom numeration and charge distribution on a molecule of benzyl alcohol.

Molecular Dynamics Simulation Parameters. A molecular dynamics simulation of a three-dimensional periodical system, such as described above, was carried using the GROMOS package.[23] A time step of 2 fs was maintained constant throughout the simulations. A long spherical cutoff radius of 2 nm and a short one of 0.8 nm were used for nonbound forces (electrostatic and van der Waals), since the critical importance of these parameters for simulation is well-known.[11] The neighboring atom list was updated every 10 time steps. The interactions of the atoms lying within the short cutoff were computed every time step, while those of the atoms that lie between the short and the long cutoff were computed only for the first time step since they remain more or less constant during the following nine time steps. Nonbound forces beyond the long cutoff were neglected. Bond length was constrained by the SHAKE method.[24]

The system was coupled to an external temperature bath[25] of 325 K (well above the transition temperature of 292 K[26]) with a pressure of 1 atm, with coupling constants of 0.1 and 0.5 ps for the temperature and pressure, respectively. Due to the anisotropy of the system, each one of the edges of the periodical three-dimensional box was independently coupled to the pressure bath.

The Ryckaert−Belleman potential[27] was used along the CH_2 chains of the lipids, since it acceptably reproduces (quite well) the gauche−trans transitions on *n*-alkane chains. In previous articles[13,14,28] the charges on the lipid molecules were divided by a factor of 2. For DMPC, Chiu et al.[22] have proposed a charge distribution that produces good results, and this was used without further modification in the present work.

Membranes with and without benzyl alcohol were simulated for 1 ns, of which the first 100 ps was discarded during equilibration of the systems. The final dimensions of the system containing three benzyl alcohols were, in nanometers, $V_x = 4.60 \pm 0.06$, $V_y = 4.68 \pm 0.06$, and $V_z = 5.77 \pm 0.12$. The deviations were computed for 900 ps of simulation. For the membrane without alcohol, the dimensions were, in nanometers, $V_x = 4.77 \pm 0.06$, $V_y = 4.40 \pm 0.06$, and $V_z = 5.91 \pm 0.12$.

3. Results and Discussion

Structure of Lipid Bilayer. A number of previous articles have dealt with structural changes in lipid bilayers induced by the presence of an anaesthetic.[1−3,7,29] From experimental data, it has been demonstrated that the presence of anaesthesia at surgical concentrations in the interior of a lipid membrane induces an increase in the fluidity of the membrane as measured by deuterium NMR. However, we note, in this regard, that the effects of the presence of anaesthetics on the fluidity of lipid membranes has only been measured at very high concentrations of anaesthetics, well above the surgical concentrations.[1]

The order parameter $-S_{CD}$ is an experimental measure of the disorder of a membrane, measured from NMR experiments. This order parameter is associated with the orientation of the hydrogens of a CH_2 group with respect to the normal to the lipid layers. Due to the fact that our simulations do not explicitly take into account the hydrogens of the CH_2 groups, the order parameter $-S_{CD}$ on the $i + 1$ CH_2 was defined as the unitary vector normal to the vector defined from the i to the $i + 2$ CH_2 group and contained in the plane formed by the groups i, $i + 1$, and $i + 2$. As a consequence, the $-S_{CD}$ on the ith CH_2 was defined as follows:

$$-S_{CD} = \frac{3\cos^2(\theta) - 1}{2} \tag{1}$$

where θ is the angle subtended by the unitary vector defined above and the Z axis. Note that $-S_{CD}$ can adopt any value in a range from -0.5 (parallel to the lipid/water interface) to 1 (oriented along the normal to the membrane).

In this regard, Turner and Oldfield[1] reported experimental values for the hydrocarbon chain quadrupole splitting obtained from NMR experiments of a DMPC membrane in its liquid crystalline state in the absence and presence of anaesthesia. The deuteron quadrupole splitting is related to the order parameter $-S_{CD}$ as follows:[30]

$$\Delta\nu_Q = -\frac{6}{8}\left(\frac{e^2qQ}{h}\right)S_{CD} \tag{2}$$

where eq is the electrostatic field gradient parallel to the C−D bond direction in the laboratory coordinate frame, e is the electric charge of the electron, Q is the nuclear quadrupolar moment, and h is the Planck constant. The deuteron quadrupole constant (e^2qQ/h) has been found to be 170 kHz for paraffin

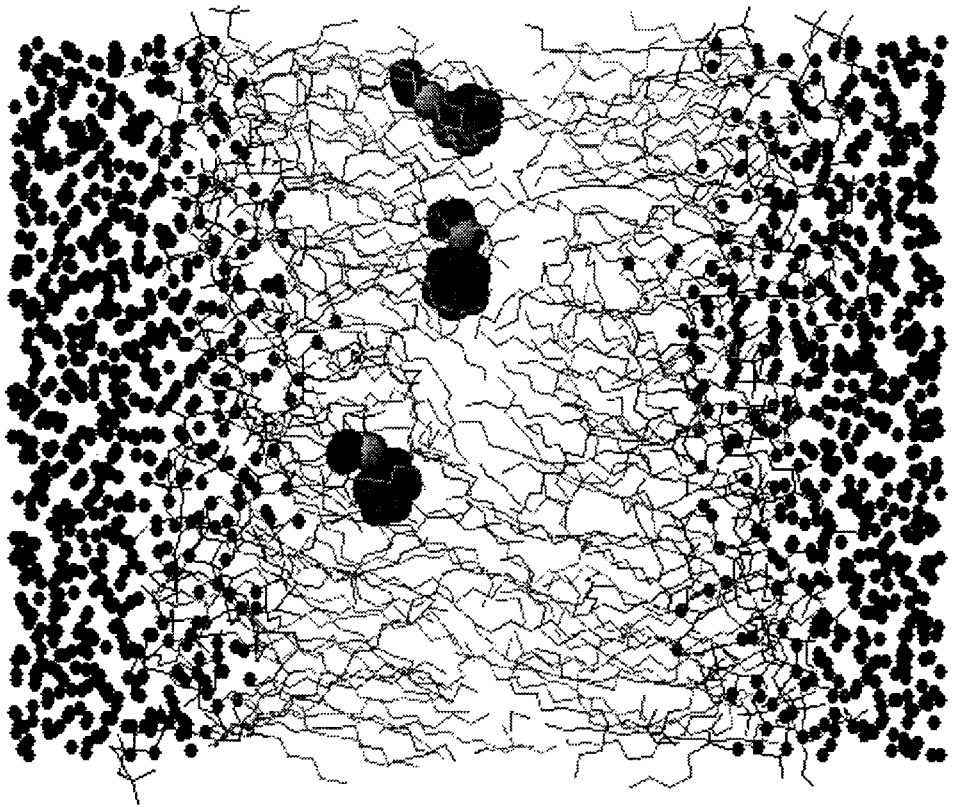

Figure 3. Snapshot of the bilayer including three benzyl alcohol molecules.

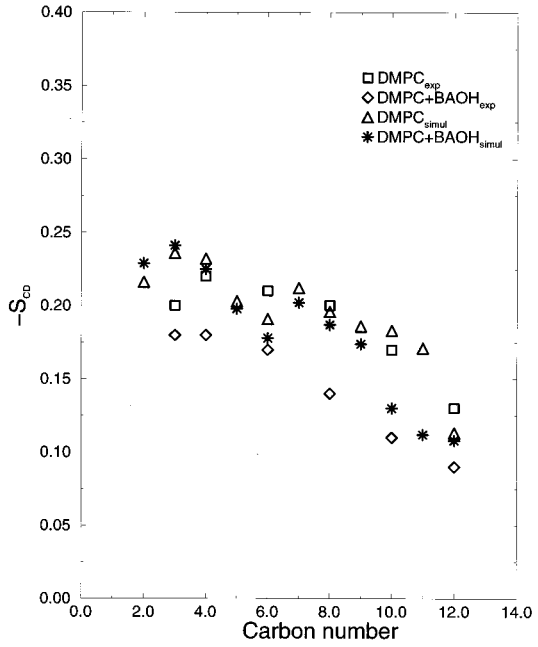

Figure 4. Order parameter along the hydrocarbon tails of a DMPC molecule, averaged over both tails.

chains.[31] Taking this value as the deuteron quadrupole constant, we obtained the order parameter along the hydrocarbon chains of the DMPC molecule from the experimental data reported by Turner and Oldfield[1] in the presence and absence of anesthetics. Figure 4 displays both experimental and simulation data. Figure 4 shows very good agreement between the simulation and experimental data for DMPC in the absence of anaesthesia, although when anaesthesia was introduced in the membrane, a diminution in the order parameter was measured for the terminal CH_2 groups of the lipid tails.

Experimentally, it has been reported[1] that the presence of the anaesthetic benzyl alcohol inside the membrane uniformly increases the disorder in the lipid tails, although this can only be observed when the concentration of alcohol is much higher than that corresponding to surgical conditions. At surgical concentrations, almost no variation was measured in the order parameter along the lipid chains.[1] Our simulations reproduced this trend, since no variation in the order parameters along the tails was observed except for the terminal carbons of the lipid tails, in which they diminished slightly and showed a tendency very similar to the experimental data measured by Turner and Oldfield[1] at higher concentration of anesthetic.

These results can be easily explained from Figure 5, in which the distribution of CH_2 and the center of mass of the alcohol molecules were displayed across the membrane. From Figure 5 we observe how the alcohol is confined to a region populated by carbons 9−12. As a consequence of this interaction between alcohol and the CH_2 groups, some perturbation in the order parameters of these carbons is to be expected, with the order parameters for the first atoms of the lipid tails, in which no carbon−alcohol interactions have been detected, remaining intact. If we could extend the trajectory length of our simulations, the benzyl molecules might get closer to the lipid−water interface and interact with the first atoms of the tails. This would lead to a reduction in the order parameter for the first atoms of the lipid tails, which is indeed shown by experimental data. When the concentration of alcohol is uniformly increased across the membrane, a diminution in the order parameters along the chain is to be expected. This would also explain the results reported by Turner and Oldfield[1] at much higher concentrations.

Concerning the surface area per lipid molecule, a value of 58.4 ± 1.4 Å^2 was measured from our simulations for a DMPC membrane in the absence of anaesthesia. This value agrees with the experimental and simulation data of DMPC membranes at temperatures above the transition temperature, which ranges

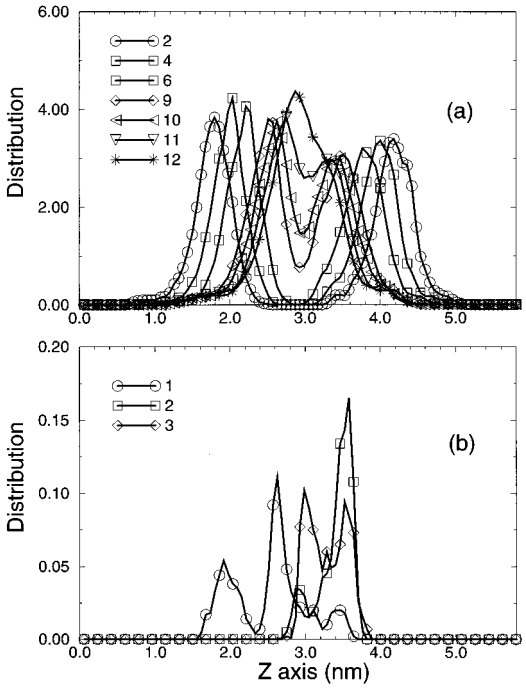

Figure 5. (a) Hydrocarbon distribution across the membrane for the lipid tails, averaged over both layers and the total trajectory length. Numbers correspond to the ethylene groups along the tail, starting from the carbonyl group. (b) Center-of-mass distribution for the three benzyl alcohol molecules (numbered 1, 2, 3) across the membrane, averaged along the total trajectory length.

from 57 to 72 Å^2,[20,22,32] depending on the technique used in the measurement. According to our simulation results, the presence of the anaesthetic in the interior of a membrane at surgical concentrations would slightly increase the surface area per lipid molecule, found to be 59.9 ± 1.4 Å^2 per lipid, which roughly corresponds to an increase of about 3% over the case in which no alcohol was dissolved in the membrane. An increase in the surface area per lipid has also been evidenced from MD simulations[5] of trichloroethylene in a dioleoylphosphatidylcholine (DOPC) lipid bilayer. However, we note that the slight increase in the area per lipid obtained from our simulations, (around 3%) lies within the statistical error associated with the MD simulations and be may be insignificant.

With the aim of pointing out the effect of anaesthetic molecules on the thickness of a lipid membrane, the thickness of the hydrocarbon region was defined from our simulations as the distance between the two maxima of the CH_2 group distributions corresponding to the first carbons of both lipid tails (atoms 17 and 34, following the atom numeration of Figure 1). Thus, the thickness of the hydrocarbon region measured from our simulations was 2.65 nm in the presence and 2.70 nm in the absence of benzyl alcohol. From our simulations, therefore, we conclude that the presence of anaesthetics at surgical concentrations does not introduce significant variations on the thickness of the hydrocarbon region of lipid membrane. These results are in very good agreement with the experimental NMR data obtained by Turner and Oldfield,[1] in which a value of 2.5 nm was estimated for the hydrocarbon region of a DMPC membrane at 311 K in the absence of benzyl alcohol, and no variation in membrane thickness was detected at surgical concentrations of anaesthesia inside of the membrane.

As regards the distributions of ammonium $N(CH_3)_3$, phosphate, and water across the membrane (Figure 6), we conclude that the presence of anaesthetics in the interior of the membrane does not perturb these distributions in any way.

Figure 6. Atom distribution across the membrane (in atoms/nm^3).

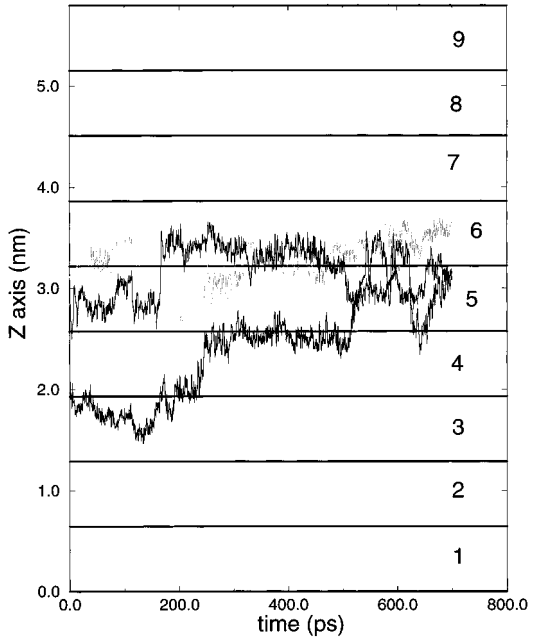

Figure 7. Benzyl alcohol motion along the *Z* axis perpendicular to the membrane surface. The numbers indicate the slabs in which the periodical computing box was divided along the *Z* axis.

Diffusion and Orientation of Benzyl Alcohol in the Interior of the Membrane. MD simulation provides valuable information regarding the dynamic properties of the benzyl alcohol confined in the interior of the hydrophobic core of the lipid membrane.

Figure 7 displays the motion of three benzyl alcohols for 900 ps of simulation in the interior of a lipid membrane of DMPC. For this purpose, the periodical computing box was divided into nine slabs of equal thickness (roughly 0.64 nm each), along the axis normal to the lipid/water interface. Slab 5 corresponds to the middle of the lipid bilayer. From this figure, we conclude

that the motion of anaesthetic molecules is clearly confined to the interior of the hydrophobic region (slabs 4−6), and they never abandon this region for other zones much closer to the lipid/water interface (slabs 2, 3, 7, and 8). This observation is consistent with the distribution of the *z* positions of the center of mass of the benzyl alcohol molecules (Figure 5), which are clearly concentrated in the innermost part of the bilayer.

As regards the rotational diffusion of the benzyl alcohol molecules, we define a unitary vector, $\vec{u}$, from atom 1 to 4 on the benzene ring (following the atom numeration in Figure 2). From the rotation of this vector along the trajectory, we obtain the $\langle P_2(t)\rangle$ function defined as follows:

$$\langle P_2(t)\rangle \equiv \langle (3\cos^2\theta(t) - 1)/2\rangle \quad (3)$$

In eq 3, $\cos\theta(t) = \vec{u}(t)\cdot\vec{u}(0)$ where $\vec{u}(0)$ describes the orientation of this unitary vector at some initial time and $\vec{u}(t)$ is the unitary vector after time *t* has elapsed. The average in eq 3 refers to the choice of the origin for the time lapse *t*, along the simulated trajectory (and a further average is carried out for the benzyl alcohol molecules that are present). This function is related to ESR and other dynamic properties. To characterize the decays of $\langle P_2(t)\rangle$, one must consider that it may have a nonzero asymptote or baseline. In practice, we fit $\langle P_2(t)\rangle$ to a sum of exponential terms plus a baseline by a nonlinear least-squares procedure, i.e.,

$$\langle P_2(t)\rangle = a_0 + \sum_{i=1}^{n} a_i \exp(-t/\tau_i) \quad (4)$$

where τ_i corresponds to each one of the correlation times and a_i to the amplitude associated with the time τ_i. In the most cases, at least two exponentials are required to fit eq 4. The individual value of each τ_i is not of great relevance. Indeed, the rotational relaxation time is characterized by a single, mean relaxation time, τ_{mean},[33] defined as

$$\tau_{\text{mean}} = \frac{\sum_{i=1}^{n} a_i \tau_i}{\sum_{i=1}^{n} a_i} \quad (5)$$

We have noticed that while the individual a_i's and τ_i's are quite sensitive to fitting details, τ_{mean} is a more robust parameter.

Applying the treatment described above to the benzyl alcohols in our simulations, and taking into account the three molecules along the whole trajectory, we obtained an average value (over the three molecules) for τ_{mean} of 5.2 ps. This value is similar to the 25 ps obtained by simulation, corresponding to the relaxation time of benzene in the interior of a DMPC membrane at 320 K.[12] An experimental value of 20 ps has been reported for di-*tert*-butyl nitroxide in dipalmitoyllecitin bilayers at 323 K,[34] although this is not directly comparable with our result for the above-described reasons.

Moreover, by simulation we can obtain valuable information regarding the dynamic properties of penetrating molecules at different depths within the membrane. For that purpose, we split the trajectory into shorter subtrajectories, so that a molecule would not pass from one slab to an adjacent one. In this regard, we estimate from Figure 7 that any benzyl alcohol remains in the same slab for roughly 50 ps, which is why we estimated

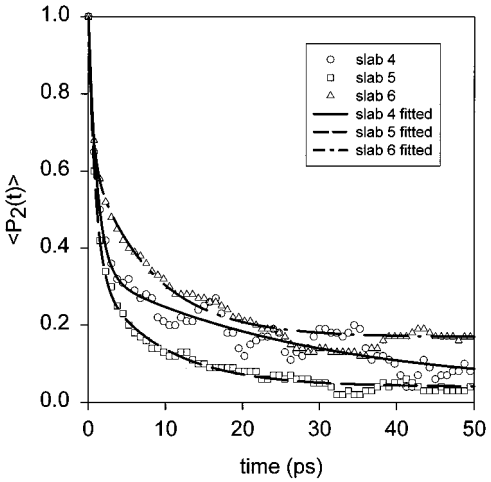

Figure 8. $\langle P_2\rangle$ decay as a function of the position in the interior of the membrane. Slab 5 corresponds to the center of the hydrocarbon region.

the dynamic properties related to the benzyl alcohol at different depths and, particularly, the $\langle P_2(t)\rangle$ function during this period of time.

Some results are shown in Figure 8, where slab 5 corresponds to the middle of the lipid bilayer. From the fit to a double exponential, we obtained mean relaxation times of 8.1, 3.4, and 4.7 ps, corresponding to slabs 4, 5, and 6, respectively. According to the symmetry of the system, the results at slabs 4 and 6 should be the same. (The observed deviation may be an artifact.) Anyway, taking an average of 6.4 ps for slabs 4 and 6, we observe that the relaxation time increases substantially, by a factor of about 2, when we approach the region populated by lipid heads (slabs 4 and 6) compared to that observed in the middle of the hydrocarbon region (slab 5). Unfortunately, no experimental data regarding this point are available for our numerical results to be compared.

For the translational diffusion coefficient of benzyl alcohol in the interior of the hydrocarbon region, we focused our interest on the lateral diffusion coefficient $D_{t,xy}$, principally because the mobility of the alcohol molecules in the *z* direction is barely noticeable during simulation. (Furthermore, the transversal diffusion coefficient, $D_{t,z}$ must be strongly position dependent.) Hence, the translational diffusion coefficient $D_{t,xy}$ parallel to the face of the lipid bilayer was computed as follows:

$$D_{t,xy} = \frac{1}{4t}\langle (x(t) - x(0))^2 + (y(t) - y(0))^2\rangle = \frac{1}{4t} r_{xy}^{\,2}(t) \quad (6)$$

where $x(0)$, $y(0)$ and $x(t)$, $y(t)$ are respectively the initial and final coordinates of the center of mass for a molecule of benzyl alcohol, after a time *t*. The averages refer to all the molecules and times. In our case, we computed the average for the three benzyl alcohols, considering a different starting position along the trajectory for each benzyl alcohol molecule.

From the slope of the time dependence of the mean-square displacement of the three benzyl alcohols, we estimated a translational diffusion coefficient of $(5.72 \pm 0.03) \times 10^{-5}$ cm^2 s^{-1}. This value is 1 order of magnitude higher than the experimental data of benzene in egg lecithin films[35] (2.0×10^{-6} cm^2 s^{-1}) and also higher than simulation results for benzene in a DMPC membrane,[12] which range from 0.5×10^{-6} to 2.0×10^{-6} cm^2 s^{-1}. This difference of 1 order of magnitude could be attributed to the time scale of our simulations. The behavior is not purely diffusive, and as a consequence, the diffusion constant $D_{t,xy}$ would be larger than expected. Although we indeed evaluate $D_{t,xy}$ from the linear plot of $r_{xy}^2(t)$, as in eq 6,

this plot may still be linear, with an abnormally high slope, when nondiffusive contributions are present. In addition, it has also been reported[36,37] that for simulations in which the hydrogens have not been taken into account in an explicit manner along the lipid chains (as in our case), artificially high diffusion rates are obtained from simulation. Furthermore, we must point out that, due to the long period of time spent by the molecules in the middle of the lipid bilayer, translational coefficients higher than the experimental ones are to be expected, since the contribution from the slower diffusivity in the vicinity of the lipid−water interface is not present in our simulation results. (We are grateful to a referee for providing this further explanation.)

By splitting up the trajectory for each benzyl alcohol into shorter subtrajectories of 50 ps each, we have been able to estimate the translational diffusion coefficient $D_{t,xy}$ of these penetrating molecules at different depths in the interior of the hydrocarbon region. From the analysis, we obtained the following values for the diffusion coefficient $D_{t,xy}$: $(1.163 \pm 0.012) \times 10^{-5}$, $(8.29 \pm 0.04) \times 10^{-5}$, and $(3.329 \pm 0.013) \times 10^{-5}$ cm^2 s^{-1}, corresponding to slabs 4, 5, and 6, respectively, where slab 5 corresponds to the middle of the hydrocarbon region. From the results of our simulations, the anisotropy in the interior of the lipid membranes is clear. This is in good qualitative agreement with the experimental data for di-*tert*-butyl nitroxide[34] in the sense that the diffusion coefficient shows the same tendency in both cases, increasing from regions close to the lipid heads (slabs 4 and 6) toward the middle of the hydrocarbon region by a factor of roughly 4 (this value being obtained as a mean of the value obtained in layers 4 and 6 of our simulations). This increase in translational diffusivity is coherent with that found for rotational diffusion, and the factor by which it increases is nearly the same. Roughly speaking, the situation is as if the viscosity in the innermost part of the membrane were 4 times smaller than in the adjacent hydrocarbon layers. From another point of view, this increase in the diffusion coefficient is strongly associated with the variations in the free volume accessible to penetrating molecules across the bilayer, such as has been reported for DPPC and DMPC membranes.[12,38]

In addition to the orientational dynamics of the embedded molecules, the orientational distribution is interesting in itself. The orientation of the benzyl alcohol molecules can be expressed by means of three mutually perpendicular vectors fixed in the molecule. These are (1) vector from atom 1 to atoms 4 and 7 within the aromatic ring vector, (2) from atom 2 to 6, again within the aromatic ring vector, and (3) perpendicular to the ring. From our molecular dynamics trajectory, we have evaluated the orientational distribution of each of these three vectors with respect to the Z axis normal to the bilayer.

Rather than the angle, θ, between each one of the molecular vectors and Z, we take as the angular variable $c \equiv \cos\theta$. In terms of this, the angular distribution, $g(c)$, corresponding to uniformly random orientation would be flat (i.e., $g(c) =$ constant). In Figure 9 we present the results for $g(c)$ for the three molecular vectors. It is clear that the 2−6 vector is orientationally indifferent, with a nearly flat $g(c)$. On the other hand, the third (normal) vector displays a significant preference to be orientated perpendicularly to the bilayer. In this situation the benzene ring lies parallel to the bilayer plane, which is perhaps the preferred orientation for benzyl alcohol molecules placed in the middle of the bilayer. Finally, for vector **3**, which points perpendicularly to the benzene ring, the distribution shows a slight tendency to orientations perpendicular to the bilayer. This may correspond to benzyl alcohol molecules closer to the bilayer faces, which experience electrostatic interaction with the polar heads and alignment with the hydrocarbon chains of the lipids.

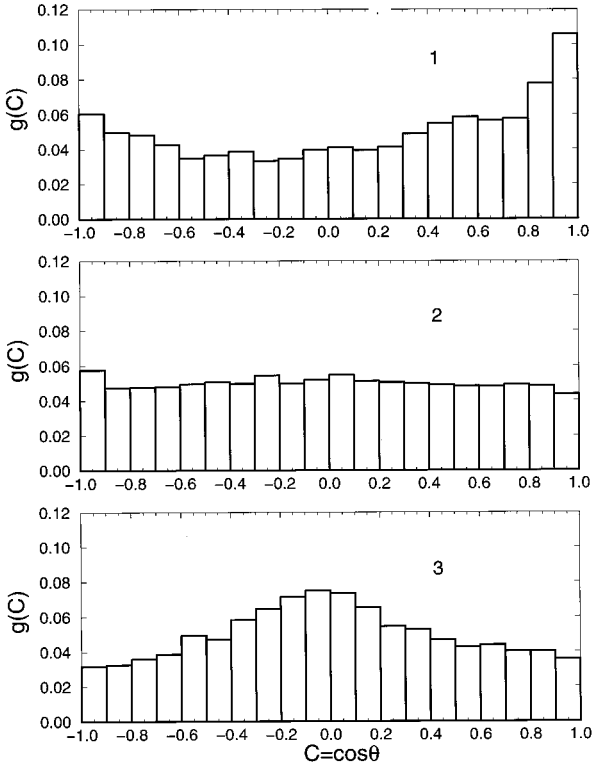

Figure 9. Orientational distribution of the benzyl alcohol molecules respect to the normal axis of the membrane: (1) vector from atom 1 to 4, attending the atom numeration of the Figure 2; (2) idem for vector from atom 2 to 6 of the Figure 2; (3) normal vector to the benzene plane.

4. Conclusion

Our simulations provide an insight into the possible perturbing effects caused by the presence of anaesthetic molecules in the structure of biological membranes. From our results, we see how the presence of anaesthetic molecules embedded in a lipid membrane at surgical concentrations does not introduce any dramatic alteration in the structure of the lipid membrane compared when anaesthetics are absent. These conclusions are reached from measuring the thickness of the hydrocarbon region, surface area per lipid molecule, and atom distribution across the membrane. The greatest perturbation is an increase in the disorder of the lipid tails at the CH_2 groups near the tail end.

Regarding the diffusivity of small molecules in the interior of a lipid membrane, it is clearly shown how it is strongly dependent on their position across the membrane. The diffusion coefficients in zones adjacent to the lipid heads are much slower than in the middle of the hydrocarbon region, as expected from free-volume considerations.

According to our MD results, the alterations in the nervous system produced by anaesthetics at low concentrations, typical of surgical levels, are hardly explained by structural changes in the lipid membranes. It is assumed, therefore, that other effects play an essential role in the mechanism of anaesthesia. For example, some effects may arise from strong anaesthetic−protein interactions, such as has been proposed in a previous set of experimental investigations.[7]

Acknowledgment. J.J.L.C. thanks the Spanish Government his financial support through a Contrato de Reincorporación de

Doctores a España. J.G.H.C. is the recipient of a predoctoral fellowship from the Comunidad Autónoma de la Región de Murcia. This work has partially been supported by the Dirección General de Investigación Científica y Técnica (Grant PB93-1132). Support was also provided by the European Commission through the program for the International Scientific Cooperation, CI1*CT94-0124.

References and Notes

(1) Turner, G. L.; Oldfield, E. *Nature* **1979**, *277*, 669.
(2) Franks, N. P.; Lieb, W. R. *J. Mol. Biol.* **1979**, *133*, 500.
(3) Ashcroft, R. G.; Coster, H. G. L.; Smith, J. R. *Nature* **1977**, *269*, 819.
(4) Ogli, K.; Tsukamoto, I.; Yokono, S.; Nogaya, J. *Ann. Acad. Med. Singapore* **1994**, *23*, 536.
(5) Huang, P.; Bertaccini, E.; Loew, G. H. *J. Biomol. Struct. Dyn.* **1995**, *4*, 725.
(6) Tonner, P. H.; Miller, K. W. *Eur. J. Anaesthesiol.* **1995**, *1*, 21.
(7) Mitchell, D. C.; Lawrence, J. T. R.; Litman, B. J. *J. Biol. Chem.* **1996**, *32*, 19033.
(8) Van der Ploeg, P.; Berendsen, H. J. C. *J. Chem. Phys.* **1982**, *76*, 3271.
(9) Alper, H. E.; Bassolino-Klimas, D.; Stouch, T. R. *J. Chem. Phys.* **1993**, *99*, 5554.
(10) Stouch, T. R. *Mol. Simul.* **1993**, *10*, 335.
(11) Alper, H. E.; Bassolino, D.; Stouch, T. R. *J. Chem. Phys.* **1993**, *12*, 9798.
(12) Bassolino-Klimas, D.; Alper, H. E.; Stouch, T. R. *Biochemistry* **1993**, *32*, 12624.
(13) Egberts, E.; Marrink, S. J.; Berendsen, H. J. C. *Eur. Biophys. J.* **1994**, *22*, 423.
(14) Marrink, S. J.; Berendsen, H. J. C. *J. Phys. Chem.* **1994**, *98*, 4155.
(15) López Cascales, J. J.; García de la Torre, J.; Marrink, S. J.; Berendsen, H. J. C. *J. Chem. Phys.* **1996**, *104*, 2713.
(16) López Cascales, J. J.; Berendsen, H. J. C.; García de la Torre, J. *J. Phys. Chem.* **1996**, *100*, 8621.
(17) Mateo, C. R.; Campillo, M. P.; Brochon, J. R.; Martínez-Ripoll, M. P.; Sanz-Aparicio, J.; Acuña, A. U. *J. Phys. Chem.* **1993**, *97*, 3486.
(18) López Cascales, J. J.; Huertas, M. L.; García de la Torre, J. *Biophys. Chem.*, in press.
(19) HyperChem, Package developed by and licensed from HyperCube, Inc., 1992.
(20) De Young, L. R.; Dill, K. A. *Biochemistry* **1988**, *27*, 5281.
(21) Berendsen, H. J. C.; Postma, J. P. M.; Van Gunsteren, W. F.; Hermans, J. Intermolecular forces. In *Intermolecular Forces*; Pullman, B., Ed.; Reidel: Dordrecht, 1981; p 331.
(22) Chiu, S. W.; Clark, M.; Balaji, V.; Subramaniam, S.; Scott, H. L.; Jakobsson, E. *Biophys. J.* **1995**, *69*, 1230.
(23) Van Gunsteren, W. F.; Berendsen, H. J. C. GROMOS: GROningen MOlecular Simulation is a software package, Biomos, Nijenborgh 4, 9747AG Groningen, The Netherlands, 1987.
(24) Van Gunsteren, W. F.; Berendsen, H. J. C. *Mol. Phys.* **1977**, *34*, 1311.
(25) Berendsen, H. J. C.; Postma, J. P. M.; Van Gunsteren, W. F.; DiNola, A.; Haak, J. R. *J. Chem. Phys.* **1984**, *81*, 3684.
(26) Yeagle, P., Ed. *The Structure of Biological Membranes*; CRC Press: Boca Raton, FL, 1992.
(27) Ryckaert, J. P.; Bellemans, A. *Chem. Phys. Lett.* **1975**, *30*, 123.
(28) Marrink, S. J.; Berkowitz, M.; Berendsen, H. J. C. *Langmuir* **1993**, *9*, 3122.
(29) Haydon, D. A.; Henry, B. M.; Levinson, S. R. *Nature* **1977**, *268*, 356.
(30) Seelig, A.; Seelig, J. *Biochemistry* **1974**, *13*, 4839.
(31) Burnett, L. J.; Muller, B. H. *J. Chem. Phys.* **1971**, *55*, 5829.
(32) Nagle, N. F. *Biophys. J.* **1993**, *64*, 1476.
(33) Venable, R. M.; Zhang, Y.; Hardy, B. J.; Pastor, R. W. *Science* **1993**, *262*, 223.
(34) Dix, J. A.; Kivelson, D.; Diamond, J. M. *J. Membr. Biol.* **1978**, *40*, 315.
(35) Rigaud, L.; Gary-Bobo, C. M.; Lange, Y. *Biochim. Biophys. Acta* **1972**, *266*, 72.
(36) Müller-Plathe, F. *J. Chem. Phys.* **1992**, *96*, 3200.
(37) Ryckaert, J. P.; Klein, M. L. *J. Chem. Phys.* **1986**, *85*, 1613.
(38) Marrink, S. J. Permeation of small molecules across lipid membranes. Ph.D. Thesis, University of Groningen, Department of Biophysical Chemistry, Nijenborgh 4, 9747 AG, Groningen, The Netherlands, 1996.